Environ Sci Pollut Res (2015) 22:6271–6279
DOI 10.1007/s11356-014-3856-x

RESEARCH ARTICLE

Mechanism of Cr(VI) reduction by *Aspergillus niger*: enzymatic characteristic, oxidative stress response, and reduction product

Yanling Gu · Weihua Xu · Yunguo Liu · Guangming Zeng · Jinhui Huang · Xiaofei Tan · Hao Jian · Xi Hu · Fei Li · Dafei Wang

Received: 13 October 2014 / Accepted: 10 November 2014 / Published online: 20 November 2014

Abstract Bioremediation of hexavalent chromium by *Aspergillus niger* was attributed to the reduction product (trivalent chromium) that could be removed in precipitation and immobilized inside the fungal cells and on the surface of mycelium. The site location of reduction was conducted with assays of the permeabilized cells, cell-free extracts, and cell debris, which confirmed that the chromate reductase was mainly located in the soluble fraction of cells. The oxidation–reduction process was accompanied by the increase of reactive oxygen species and antioxidant levels after hexavalent chromium treatment. Michaelis–Menten constant (K_m) and maximum reaction rate (V_{max}), obtained from the Lineweaver–Burk plot were 14.68 μM and 434 μM min^{-1} mg^{-1} of protein, respectively. Scanning electron microscopy and Raman spectra analyses manifested that both Cr(VI) and Cr(III) species were present on the mycelium. Fourier transform-infrared spectroscopy analysis suggested that carboxyl, hydroxide, amine, amide, cyano-group, and phosphate groups from the fungal cell wall were involved in chromium binding by the complexation with the Cr(III) and Cr(VI) species. A Cr(VI) removal mechanism of Cr(VI) reduction followed by the surface immobilization and intracellular accumulation of Cr(III) in living *A. niger* was present.

Keywords Cr(VI) reduction · *Aspergillus niger* · Reductase · Bio-immobilization · Oxidative stress · Antioxidant enzyme

Responsible editor: Philippe Garrigues

Highlights: A systematic mechanism of removal of Cr(VI) by living fungi was presented.
The removal efficiency reached above 80 % for 100 mg L^{-1} Cr (VI) solutions.
Cr(VI)-induced oxidative stress in *Aspergillus niger* was concentration-dependent.
Key functional groups and their roles in biosorption were described.

Y. Gu · W. Xu · Y. Liu · G. Zeng · J. Huang · X. Tan · H. Jian · X. Hu · F. Li · D. Wang
College of Environmental Science and Engineering, Hunan University, Changsha 410082, People's Republic of China

Y. Gu · W. Xu (✉) · Y. Liu · G. Zeng · J. Huang · X. Tan · H. Jian · X. Hu · F. Li · D. Wang
Key Laboratory of Environmental Biology and Pollution Control (Hunan University), Ministry of Education, Changsha 410082, People's Republic of China
e-mail: hnuesexwh@gmail.com

Introduction

Chromium is one of the most frequently used and toxic heavy metals, which has posed a great threat to the environment. Sources identified as contributing to the wide dissipation of Cr(VI) included chrome-plating, leather tannery, dyes and pigments, anti-corrosion agents, textiles, etc. (Contreras et al. 2011; Dong et al. 2011; He et al. 2011; Sultan and Hasnain 2007). An alarming amount of chromium wastes was discharged to the environment annually, which led to heavy environmental pollution, especially to soils and waters (Kamaludeen et al. 2003).

Among the nine valence states of Cr (ranging from −2 to + 6), Cr(VI) and Cr(III) are more significant to the environment due to their stable oxidation forms in nature. Cr(VI) compounds could cause serious injury to living organisms including allergies, irritations, and respiratory track disorders. In addition, it is a carcinogenic and mutagenic agent (Jin et al. 2014; Megharaj et al. 2003), and the toxicity is mainly resulted from the process of its reduction to Cr(V), and then Cr(V) was oxidized to Cr(VI). In this process, free radicals and reactive oxygen species (ROS) are generated (Kılıç et al. 2010). Moreover, non-biodegradable character and high solubility in aqueous environment contribute to the enduring stability, which increases the toxicity and contamination ability of this heavy metal (Garavaglia et al. 2010). By contrast,

derivates of Cr(III) are less toxic and mutagenic than Cr(VI), due to the water-insolubility at neutral pH (Mohan and Pittman 2006). Besides, Cr(III) is an essential micronutrient for humans at low concentrations to use glucose, protein, and fat for metabolism (Thacker et al. 2007). Thus, available approaches to eliminate chromium pollution in the environment are concentrated on reducing hexavalent to trivalent form.

Conventionally, physical–chemical techniques have been employed to reduce Cr(VI) such as ion exchange, sedimentation, chemical reduction, and adsorption (Krishna and Philip 2005; Xu et al. 2011). However, the methods mentioned above are limited by the disadvantages of secondary pollution along with high cost and high energy requirement (Dhal et al. 2013). Thus, novel, cost-efficient, and more environmentally friendly technologies are highly desirable.

Bioremediation technology has been suggested as a potential alternative to the conventional techniques for Cr(VI) removal (Joutey et al. 2014; Park et al. 2005a). Particularly, *Aspergillus niger* gains its popularity to tackle Cr(VI)-contaminated water. As a fungi, *A. niger* could be cheaply and readily produced in a large scale from established industrial fermentation processes as a byproduct (Park et al. 2005a, 2005b). The removal of metal ions from aqueous solution by microorganisms usually depends on the integrated mechanisms involving bioaccumulation, biosorption, and reduction processes. Present studies suggested that reduction plays a significant role in the process of hexavalent chromium removal by *A. niger* (Park et al. 2005a). Although there are extensive studies on Cr(VI) removal by *A. niger*, the precise mechanisms of reducing Cr(VI) to Cr(III) are still unclear. Besides, many researches explained the oxidative stress induced by various heavy metals in plants (Rai et al. 2005), algae (Aravind and Prasad 2005), and bacteria (Ackerley et al. 2004; Hu et al. 2005). Yet, little literature elaborated the fungal oxidative stress induced by Cr(VI). To close these knowledge gaps, more in-depth investigations are needed. In this context, it is very important to understand the adaptive changes of fungi both biochemically and morphologically in response to Cr(VI).

The objectives of this work are to study the mechanism of *A. niger* in the reduction of Cr(VI) using different experimental approaches involving biochemical, Fourier transform-infrared spectroscopy associated with Raman spectra, and Scanning electron microscopy surface analyses: (1) Reduction of Cr(VI) by various components and pretreated cell-free extracts of biomass were carried out to validate the enzyme-mediated reduction process, and the location of chromate reductase was elucidated. (2) Biochemical analyses of activity of total superoxide dismutase (T-SOD) and catalase (CAT), and the malondialdehyde (MDA) content were carried out to study the resistibility of fungi to Cr(VI)-induced free radicals. (3) The morphological changes and reduction product were studied through scanning electron microscopy (SEM). Fourier transform infrared (FT-IR) and Raman analyses were conducted to study the interactions between Cr and functional groups on fungal surface.

Material and methods

Reagents and cultivation of microorganism

All chemicals used were analytically pure grade throughout this study and used without further purification.

An axenic strain of *A. niger* (CICC41115) was purchased from the China Center of Industrial Culture Collection (Beijing, China). The cultures were grown in sterilized potato dextrose Agar medium (PDA) and Czapek Dox liquid medium.

Time-course of Cr(VI) reduction by *A. niger*

Spores (3–4 days old) incubated on PDA slants at 37 °C were used for the preparation of inocula. Experiment of Cr(VI) reduction by living-cells of *A. niger* was conducted under gyratory shaking of 150 rpm at 37 °C from 0 to 4 days in 250-mL flasks, which including 100 mL sterile Czapek Dox liquid medium, inocula, and 50 mg L^{-1} Cr(VI) using potassium chromate (K_2CrO_4) instead. The Cr(VI) stocks were filter-sterilized using 0.22-μm filters (Millipore, Bedford, MA). Aliquots of 2 mL were withdrawn every 2 h and then subjected to centrifugation (6,000 rpm for 10 min at 4 °C). The supernatants were harvested to calculate the remaining Cr(VI) and total Cr.

Resting and permeabilized cell assays

Cells of *A. niger* were grown in Czapek Dox liquid medium for 24 h and harvested by centrifugation as above. Cell pellets of *A. niger* were washed twice with 100 mM potassium phosphate buffer (PBS) (pH 7.0), and resuspended in the same buffer. Thus, the resting cells were obtained. Resting cells were treated with 10 μg mL^{-1} antifungal protein for 5 min and rinsed with PBS above to achieve membrane-permeabilized cells (Theis et al. 2003). Resting and permeabilized cell were transferred to sterile 100-mL Erlenmeyer flasks which were spiked with potassium dichromate to final concentration of 50 mg L^{-1}, respectively. Flasks were vortexed gently for 2 min and incubated at 37 °C for 6 h. At the end of incubation, aliquots of 2 mL were withdrawn and centrifuged as above; the remaining Cr(VI) was estimated from the supernatants.

Sub-cellular fractionation and localization of chromate reductase activity

Cell-free extracts (CFE) of *A. niger* were prepared by using a modified method of previously published literatures (Camargo et al. 2003; Cheng et al. 2010). Cells grown for 2 days in Czapek Dox liquid medium were harvested after centrifugation as above, washed, and resuspended in 100 mM PBS as above. Cell suspensions were placed in ice bath and disrupted using an Ultrasonic Probe (Scienta-II D) with amplitude of 40 % at 950 W with 2-s pulses and 4-s intervals for 15 min. Thus, sonicates were obtained and then centrifuged at 10,000 rpm for 30 min at 4 °C. The obtained supernatants were filtered through 0.22-μm filters to yield the CFE devoid of membrane fractions (CFE was spread onto an agar plate for testing the viability. After being cultured at 37 °C for 24 h, no colony was generated on the agar plate, indicating that the sonication treatment is an effective tool to disrupt the cells). The precipitations after centrifugation were accordingly resuspended in same volume of PBS and used for subsequent assays. CFE and cell debris were used for chromate reductase assay in order to locate the chromate reductase activity in the cells. All the assays were conducted in triplicates with freshly prepared CFE.

Chromate reductase assay

With the purpose of investigating the roles of enzyme in Cr(VI) reduction, CFE was subjected to three treatments—10 mM $AgNO_3$ at room temperature, 0.5 % sodium dodecyl sulfate (SDS) at room temperature, and heat denaturing at 95 °C for 10 min. Treated and untreated (control) CFE were used for Cr(VI) reductase tests. The initial concentration of Cr(VI) in these tests was 10 mg L^{-1}, considering the small doses CFE in actual experiment. The protein concentrations in the CFE samples were measured by the Bradford method with bovine serum albumin as the standard. Kinetics of Cr(VI) reduction by CFE was evaluated using different initial Cr(VI) concentrations ranging from 50 to 500 μM. Reaction mixtures in a total volume of 1 mL consisted of 0.4 mL CFE (0.11 mg protein) and 0.6 mL different concentrations of Cr(VI) in 50 mM PBS (pH 7.0), and they were incubated for 30 min at 37 °C. The amount of residual Cr(VI) in the reaction mixture was quantified. Michaelis–Menten equation was used to determine the Michaelis constant (K_m) and maximum velocity of the enzyme (V_{max}). K_m and V_{max} were estimated by linear regression analysis of the values obtained in the assay.

Cr(VI) effect on the antioxidant system of fungi

A. niger was treated with 0, 10, 30, 50, and 70 mg L^{-1} Cr(VI), respectively, and the treated fungal cells were used to prepare CFE by sonication as above. The protein concentrations in the CFE samples were measured as above. The CFE enzyme activities of total superoxide dismutase (T-SOD) and catalase (CAT), and the content of malondialdehyde (MDA) were measured by analysis kits (Nanjing institute of biological engineering, China).

Characterization of reduction product

To identify the character of reduction product, the fungal cells associated with the reduction product were characterized by SEM, Raman spectroscopy, and FT-IR spectroscopy. For SEM (TM3000, Hitachi, Japan) study, the fungal cells loaded with/without chromium (after 48 h incubation) were triple-rinsed to remove impurities with PBS (pH 7.0). Samples were freeze-dried overnight at −55 °C before it was examined.

For Raman spectroscopy (Labram-010, Hotiba Jobin Yvon, France) and FT-IR analyses, the fungal cells exposed to 50 mg L^{-1} Cr(VI) and without Cr(VI) were incubated for 48 h. Then, the cells were separated by centrifugation at 6,000 rpm, 4 °C for 10 min. The supernatant was abandoned while the pellets were washed with deionized water and dried in oven at 70 °C overnight. The FT-IR spectra of dried cells associated with or without reduction product in KBr phase were recorded using FT-IR spectrophotometer (IR Affinity-1, Shimadzu Corporation, Japan).

Analytical techniques

The concentration of Cr(VI) was determined by the 1,5-diphenylcarbazide method at 540 nm with UV–vis spectrophotometry (UV-2550, Shimadzu Corporation, Japan) and compared with standards Cr(VI) which was prepared with K_2CrO_4. Total Cr concentration measurement was made using flame Atomic absorption spectroscopy (TAS990, Purkinje General, China). The concentration of Cr(III) could be acquired by deducting the remained Cr(VI) from the total Cr in the supernatant (Shen et al. 2012).

The responses of *A. niger* to the Cr(VI) stress were analyzed by a one-way ANOVA test. If the statistical test was found to be significant at $p<0.05$, a Tukey's test was used to determine the difference. All the tests were conducted using the Statistical Package for Social Science (SPSS v. 18). The results shown in the figures represent the average of three independent replicate treatments. The data obtained in this study are presented as means±standard deviations.

Results and discussions

Efficiency of Cr(VI) reduction by *A. niger*

The time-course of 50 mg L^{-1} Cr(VI) reduction by the *A. niger* was shown in Fig. 1. Hexavalent chromium concentration

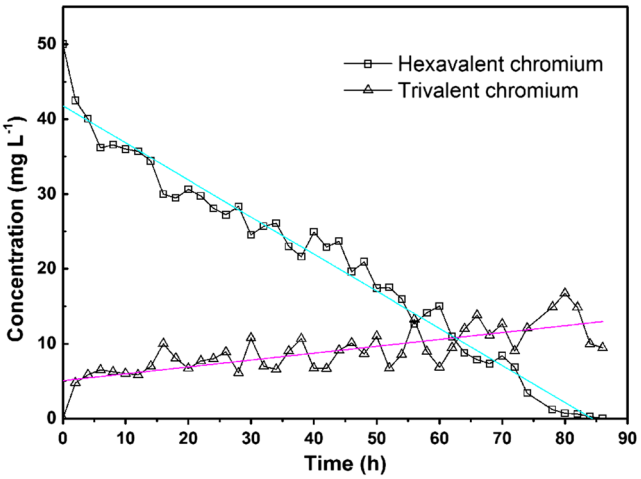

Fig. 1 Changes in Cr(VI) and Cr(III) concentrations with the initial concentration of 50 mg L^{-1} Cr(VI), at 37 °C

decreased straightly to 0 in 84 h. The fungi showed high efficiency to reduce Cr(VI) (exceeding 99 % in 84 h). Except for Cr(VI) and Cr(III), other valence states of Cr (ranging from −2 to +6) are unstable in nature , so we count the Cr(III) concentration as deducting the remained Cr(VI) from the total Cr in the supernatant. Compared with the decrease in Cr(VI), the Cr(III) gradually accumulated until the Cr(VI) vanished, and the final concentration of Cr(III) was 9.45 mg L^{-1}. The Cr(VI)-Cr(III) graph showed that *A. niger* could significantly remove Cr(VI), and reduction of part of Cr(VI) by *A. niger* that was verified by the Cr(III) remained in the supernatant. However, whether the missing Cr(VI) was reduced or adsorbed was still unclear, which will be discussed in the following sections.

Characterization of chromate reductase activity in *A. niger*

Chromate reductase assays were carried out using resting and permeabilized cells of *A. niger* by exposing the cells to 50 mg L^{-1} Cr(VI) for 6 h at 37 °C. Table 1 showed the degree of reduction of Cr(VI) upon exposure of resting and permeabilized cells of *A. niger* to Cr(VI). As shown in this table, the resting cells reduced 42.2 % Cr(VI), while degree of reduction of 46 % Cr(VI) was observed by permeabilized cells of *A. niger*. The results of resting and permeabilized cell assays suggested that the enhanced permeabilization does not work in the increase of degree of reduction.

Table 1 Degree of reduction of 50 mg L^{-1} Cr(VI) by different cell components

Cell components	Reduction ratio of Cr(VI) (%)
Resting cells	42.2±2.8
Permeabilized cells	46.0±2.0
Supernatant metabolites	6.1±0.9
Cell-free extract	59.0±3.4
Cell debris	2.1±0.4

Fungi was disrupted and separated into cell debris and CFE. The reduction ability of these components to Cr(VI) was analyzed, respectively. As shown in Table 1, when 50 mg L^{-1} Cr(VI) were introduced into the CFE, degree of reduction of Cr(VI) attained 59 % within 6 h. The result confirmed that Cr(VI) reduced by *A. niger* is mainly dependent on CFE. Like most bacterial cases, chromium reductase activity is related to the intracellular fraction (Myers et al. 2000; Ravindranath et al. 2011). Conversely, no significant change of the Cr(VI) concentration was observed when cell debris were introduced, which denoted that the cell debris could not contribute to reduction of Cr(VI) directly, and the 2.1 % degree of reduction by cell debris may be on account of physical absorption. The 6.1 % Cr(VI) degree of reduction by supernatant metabolites suggests that a small part of Cr(VI) could be reduced by some compositions in metabolites.

CFE was further suffered from 95 °C heat and protein denaturants, in order to check out whether the reduction process was enzyme-mediated or not. As shown in Fig. 2, the reduction of Cr(VI) can be terminated by heat denaturalization. It indicated that the reduction of Cr(VI) was attributed to Cr(VI) reductase or some unclear heat-sensitive reductants in the CFE, which contributed to the Cr(VI) reduction. To confirm the character of reduction substances, we treated CFE with other protein denaturants at room temperature. Figure 2 exhibited that both heavy metals (Ag^{+}) and surfactants (SDS) may significantly affect or even terminate the effective reduction of Cr(VI). A control experiment of untreated CFE was also conducted. The results indicated that the reduction of Cr(VI) by CFE of *A. niger* was enzyme-mediated.

In order to evaluate the rate of Cr(VI) reduction, the kinetics of Cr(VI) reduction at different Cr(VI) concentrations was

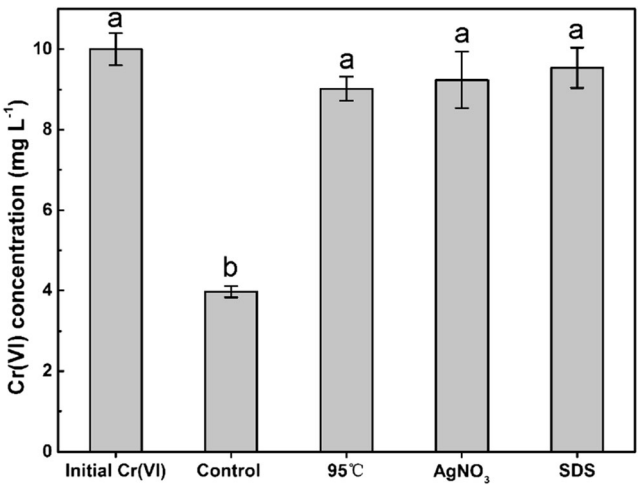

Fig. 2 The remaining Cr(VI) concentrations after reduction by CFE suffered from 95 °C heat and protein denaturants. Different *letters* indicate significant differences between different treatments ($p<0.05$)

studied. The saturation kinetics of Cr(VI) reduction by the CFE of *A. niger* fit the hyperbolic Eq. 1:

$$V_0 = \frac{V_{\max}[S]}{K_m + [S]} \quad (1)$$

The Michaelis–Menten constant (K_m) was 434 μM and V_{max} was 14.68 μM min^{-1} mg^{-1} protein.

Cr(VI)-induced oxidative stress in fungal cells

In Fig. 3a, we could observe that the MDA content increases with the increase of Cr(VI) concentration, and the increase of MDA content is especially obvious at 70 mg L^{-1} Cr(VI) ($p<0.05$).

As shown in Fig. 3b, the T-SOD activity increases with the increase of Cr(VI) concentration from 0 to 30 mg L^{-1} and subsequently decreases at the Cr(VI) concentration ranging from 30 to 70 mg L^{-1}, which emerged a bell-shaped concentration–response curves.

CAT activity is shown in Fig. 3c; a significant increase appears when Cr(VI) concentration increases from 0 to 10 mg L^{-1} ($p<0.05$), and there is no obvious variation between the CAT activity at the Cr(VI) concentrations of 10, 30, and 50 mg L^{-1} ($p>0.05$). And then CAT activity descends at 70 mg L^{-1} Cr(VI) concentration, which is similar to the bell-shaped concentration–response curves of T-SOD.

Ackerley et al. (2004) elaborated the ROS toxicity to biomass induced by heavy metals (Ackerley et al. 2004). The ROS includes singlet oxygen ($^1O_2$), superoxide (O^{2-}), hydrogen peroxide (H_2O_2), and hydroxyl radical ($^{\cdot}OH$). The process of ROS generation induced by heavy metals is oxidative stress. Cr(VI) is toxic to cellular processes by both enzymatic and nonenzymatic mechanisms, with the production of ROS in reduction process. This process may be a major factor in causing damage to cellular components, including DNA and protein (Hu et al. 2005). Generally, in this case, biomass could engender stress response to resist the ROS damage by producing more corresponding enzymes, such as SOD (to convert superoxide to hydrogen peroxide) and CAT (to convert hydrogen peroxide to water and oxygen) (Baptista et al. 2009). Besides, MDA content was broadly available to indicate lipid peroxidation, which was related to the production of O^{2-}. The evaluation of MDA levels represents the free-radical-generating capacity of the microorganism via metal ions stimulating (Zeng et al. 2012). For the purpose of understanding the fungal resistance to Cr(VI), we studied the relationship between the Cr(VI) concentration and the antioxidant system of *A. niger*.

In the current research, increased free radical generation was found in *A. niger* under Cr(VI) stress as indicated by the MDA product, which is similar to the effect of heavy metals on higher plants (Dhir et al. 2004; Saradhi and Mohanty 1993). In Fig. 3a, we could see that MDA levels rose up steadily with the increase of Cr(VI) concentration, which

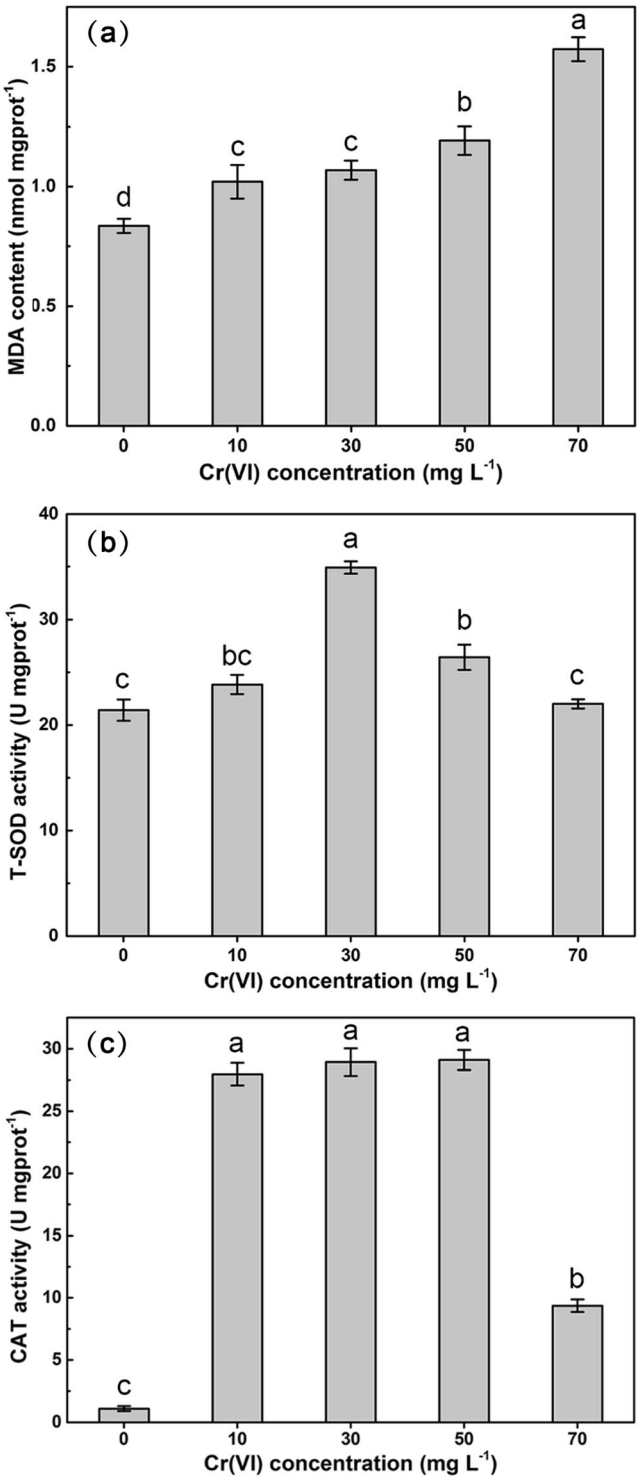

Fig. 3 Effects of Cr(VI) on fungal oxidative stress system under different initial Cr(VI) concentrations; **a** MDA content; **b** T-SOD activity; **c** CAT activity. Different *letters* indicate significant differences between treatments with different Cr(VI) concentrations ($p<0.05$)

suggested that the generation of free radical was concentration-dependent. In comparison with the MDA at 70 mg L^{-1} of Cr(VI), MDA at lower Cr(VI) concentration presented no evident distinction ($p<0.05$). The generation and accumulation of Cr(VI)-induced ROS would induce fungi to produce more antioxidant enzymes to protect their own cells from the damage of free radicals. As shown in Fig. 3b and c, T-SOD and CAT showed the similar trend which emerged as bell-shaped concentration–response curves. Our result was in consistent with the previous research which described the stress responses of *Phanerochaete chrysosporium* as bell-shaped curves (Zeng et al. 2012). The decrease of T-SOD and CAT at higher Cr(VI) concentration was attributed to the excessive ROS accumulation, leading to cell death and antioxidant system breakdown. And at high Cr(VI) concentration, the interaction between excess metals and cellular components engendered ROS overproduction, leading to cytotoxicity outbreak. According to the observed feature of cellular damage (MDA level) and antioxidant enzyme activity, we could conclude that the tolerance of *A. niger* to Cr(VI) mainly depends on its ability to avoid oxidative stress.

Characterization of the reduction product

SEM analyses

In order to get further insight into the character of reduction product species, the SEM studies of fungal cells, grown in the absence and presence of 100 mg L^{-1} Cr(VI) in Czapek Dox liquid medium, were undertaken and the results are presented in Fig. 4. SEM micrographs of untreated mycelia were regular and integrated, while the mycelia upon treatment with Cr(VI) showed distinct changes. The obvious changes in morphology indicated that cells were suffered from toxicity of Cr(VI). And also, we could see the crystal attached to the surface of fungal cells in Fig. 4, which indicated the adsorption process. This result is consistent with the previous study which demonstrated that particles on the cells surface of *A. niger* were Cr(VI) by SEM micrographs combined with EDAX spectra (Khambhaty et al. 2009). We could confirm that the crystal was one of the chromium compounds.

FT-IR and Raman analyses

Figure 5a shows FT-IR spectra of the pristine *A. niger* and biomass loaded with chromium. The complex nature of the biomass was indicated by a number of absorption peaks in the control sample (Fig. 5a (I)). The band around 3,359 cm^{-1} is indicative of the existence of the –OH groups, whereas the C=O groups stretching at the band 1,740 cm^{-1} demonstrated the presence of –COOH. The band at 2,928 cm^{-1} is representative of –CH stretching including $–CH_3$ and $>CH_2$ functional groups attributed to fatty acids found in fungal membrane phospholipids. The moderately strong absorption bands at 1,647 and 1,546 cm^{-1} were observed as amide I and amide II respectively, whereas band at 1,035 cm^{-1} indicated the presence of P–O alkyl (phosphorous compounds) of polysaccharides (Yee et al. 2004). The band located at 2,360 cm^{-1} indicated the amine group of proteins. Since –CN stretching can also appear around the wavelength of 1,350–1,000 cm^{-1}, the weak peaks at 1,074 and 1,313 cm^{-1} were identified as the

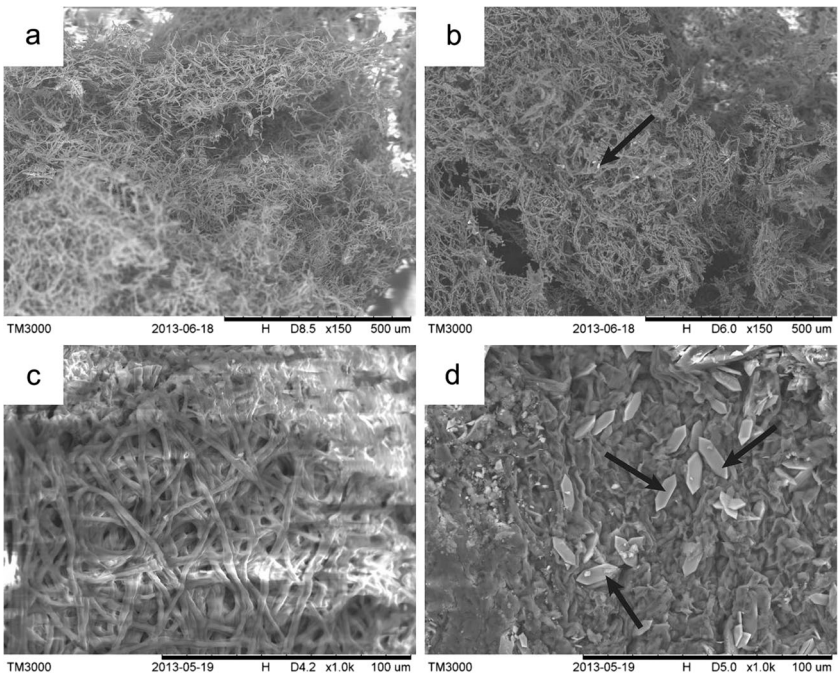

Fig. 4 SEM micrographs of *A. niger* grown in the absence and presence of 100 mg L^{-1} Cr(VI); **a** grown in the absence of Cr(VI)× 150; **b** grown in the presence of Cr(VI)×150; **c** grown in the absence of Cr(VI)×1,000; **d** grown in the presence of Cr(VI)×1,000

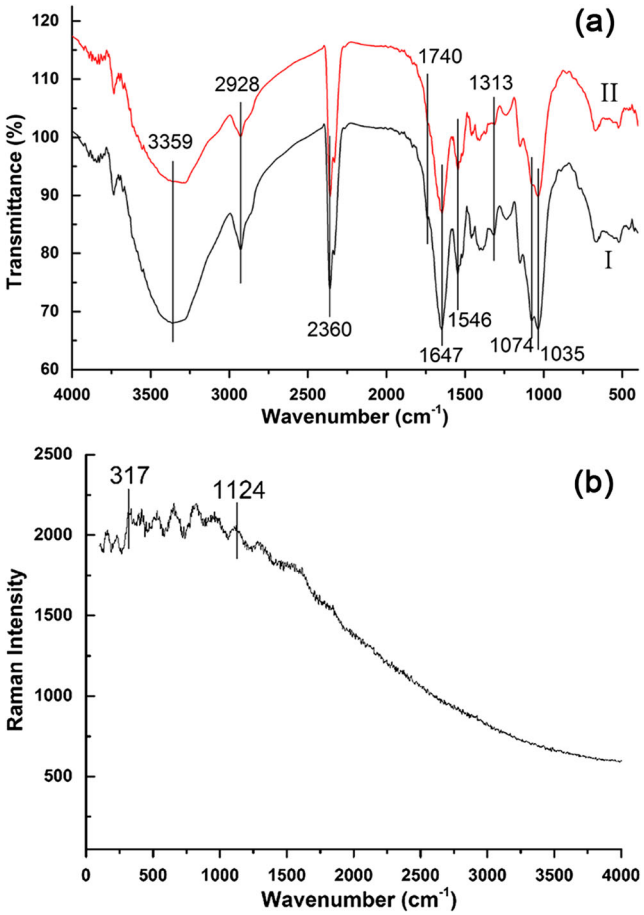

Fig. 5 **a** FT-IR spectra of (I) the pristine *A. niger* and (II) *A. niger* loaded with chromium, **b** Raman spectroscopy of *A. niger* loaded with Cr(VI)

–CN stretching vibration of protein fractions (Bai and Abraham 2002).

Figure 5a (II) showed the fluctuation in the spectrum of the biomass after sorption of chromium. The decrease in width and intensity of the band around 3,359 cm^{-1} and the weakness of the band at 1,740 cm^{-1} with respect to the control spectrum collectively illustrated that hydroxyl and carboxyl groups contributed to adsorption. The decrease of –CH groups at band 2,928 cm^{-1} corresponds to the reduction of phospholipid. The spectral analysis showed that there were several remarkable decreases in the absorption intensity of –NH (2,360 cm^{-1}) and –CN (1,074 and 1,313 cm^{-1}) after Cr adsorption, which indicated that the –NH and –CN group of protein were involved in Cr(VI) binding. Similarly, obvious weakness occurred at band 1,035 cm^{-1} suggesting that $-PO_4^{3-}$, which consisted in polysaccharide, participated in Cr(VI) binding. As major compositions of fungal cell membrane, phospholipid, protein, and polysaccharide played important roles in the Cr(VI) biosorption. The intensity of the peak at 1,647 and 1,546 cm^{-1}, which moderately shrunk, indicated that amide I and amide II were involved in Cr(VI) binding in some way. Though various functional groups were expressed in different experimental conditions, our results were basically in line with the reported articles that many potential "ligands" including carboxylate, amine, phosphate, hydroxyl, sulfhydryl, and other functional groups were the sites of metal uptake (Kapoor and Viraraghavan 1997). In present study, functional groups such as carboxyl, hydroxide, amine, amide, cyano-group, and phosphate were responsible for Cr(VI) binding as ligands. The identification of these functional groups in the FT-IR spectrum of pristine and Cr(VI)-pretreated biomass is indicative of their contribution to the biosorption of chromium by the *A. niger* biomass.

As a complementary analysis, Raman spectroscopy test of fungi supplement with Cr(VI) was conducted. In Fig. 5b, a broad and high peak was observed, from about 317 to 1,124 cm^{-1}, with several unconsidered fluctuation. A series of published literatures demonstrated that Cr in different valence states has different absorption peaks in Raman spectra. Cr(VI) compounds have characteristic peaks in area around 500, 900, and 1,000 cm^{-1}, whereas Cr(III) compounds have distinctive bands around 300 and 600 cm^{-1} (Kikuchi et al. 2005; Vaskova and Kolomaznik 2013). This indicated that both of Cr(VI) and Cr(III) compounds were present on the mycelium. In conclusion, the FT-IR and Raman analyses confirmed the adsorption effect of Cr(VI) by *A. niger*. So we

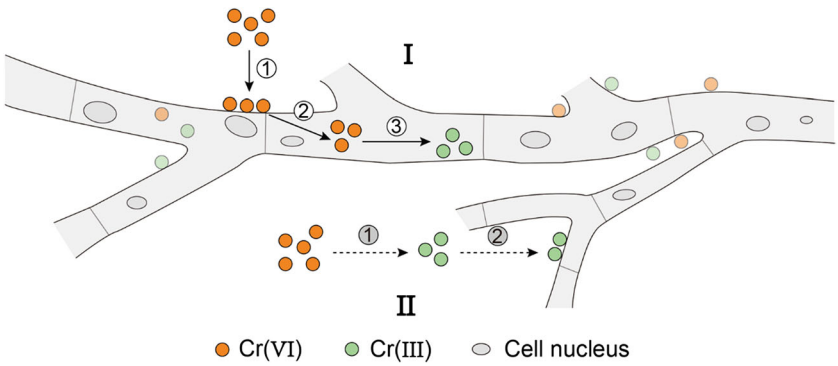

Fig. 6 Conceptual diagram of chromium removal mechanism by *A. niger* involving two simultaneous processes. Process I including: (*1*) Cr(VI) in solution was adsorbed on the surface of fungal cells; (*2*) Cr(VI) accessed into cells due to the high penetration of Cr(VI); (*3*) Cr(VI) was reduced to water-insoluble Cr(III); Process II including: (*1*) A small part of Cr(VI) in solution was reduced to Cr(III) by cell secretions; (*2*) the reduced Cr(III) was adsorbed on the surface of cells

conclude that part of Cr(VI) was reduced to Cr(III), and another part was absorbed on the surface of cells.

Mechanisms of Cr(VI) reduction by *A. niger*

Through series of tests above, a cellular and enzymatic mechanism of fungi on reduction of Cr(VI) is present in Fig. 6.

In general, the Cr(VI) reduction mechanism by *A. niger* could be divided into two parts: (1) Cr(VI) in solution was immobilized by coordination with the functional groups on the surface of fungal cells, including carboxyl, hydroxide, amine, amide, cyano-group, and phosphate as depicted above, and the Cr(VI) complex was generated; a small part of Cr(VI) in solution was reduced to Cr(III) by some reduction substances in cell secretions. Furthermore, extracellular Cr(VI) complex and Cr(III) were immobilized on the surface of fungal cells, which can be seen in the SEM micrographs. (2) Cr(VI) accessed into cells due to its high penetration, and then Cr(VI) was reduced to water-insoluble Cr(III) species, which accumulated as precipitation; however, intracellular penetration of Cr(III) is rather impossible (Smutok et al. 2011), so Cr(III) species were immobilized in cells.

Acknowledgments The authors would like to thank financial support from the National Natural Science Foundation of China (51108167), Research Fund for Doctoral Program of Higher Education of China (20100161120011), the Hunan Provincial Natural Science Foundation of China (11JJB003), and the Fundamental Research Funds for the Central Universities, Hunan University.

Reference

Ackerley DF, Gonzalez CF, Keyhan M, Blake R 2nd, Matin A (2004) Mechanism of chromate reduction by the *Escherichia coli* protein, NfsA, and the role of different chromate reductases in minimizing oxidative stress during chromate reduction. Environ Microbiol 6: 851–860

Aravind P, Prasad M (2005) Cadmium-induced toxicity reversal by zinc in *Ceratophyllum demersum* L. (a free floating aquatic macrophyte) together with exogenous supplements of amino- and organic acids. Chemosphere 61:1720–1733

Bai RS, Abraham TE (2002) Studies on enhancement of Cr(VI) biosorption by chemically modified biomass of *Rhizopus nigricans*. Water Res 36:1224–1236

Baptista P, Ferreira S, Soares E, Coelho V, Bastos ML (2009) Tolerance and stress response of *Macrolepiota procera* to nickel. J Agric Food Chem 57:7145–7152

Camargo F, Okeke B, Bento F, Frankenberger W (2003) In vitro reduction of hexavalent chromium by a cell-free extract of *Bacillus* sp. ES 29 stimulated by Cu^{2+}. Appl Microbiol Biotechnol 62:569–573

Cheng Y, Yan F, Huang F, Chu W, Pan D, Chen Z, Zheng J, Yu M, Lin Z, Wu Z (2010) Bioremediation of Cr (VI) and immobilization as Cr (III) by *Ochrobactrum anthropi*. Environ Sci Technol 44:6357–6363

Contreras E, Ferro Orozco A, Zaritzky N (2011) Biological Cr (VI) removal coupled with biomass growth, biomass decay, and multiple substrate limitation. Water Res 45:3034–3046

Dhal B, Thatoi H, Das N, Pandey B (2013) Chemical and microbial remediation of hexavalent chromium from contaminated soil and mining/metallurgical solid waste: a review. J Hazard Mater 250: 272–291

Dhir B, Sharmila P, Saradhi PP (2004) Hydrophytes lack potential to exhibit cadmium stress induced enhancement in lipid peroxidation and accumulation of proline. Aquat Toxicol 66:141–147

Dong X, Ma LQ, Li Y (2011) Characteristics and mechanisms of hexavalent chromium removal by biochar from sugar beet tailing. J Hazard Mater 190:909–915

Garavaglia L, Cerdeira SB, Vullo DL (2010) Chromium (VI) biotransformation by β-and γ-Proteobacteria from natural polluted environments: a combined biological and chemical treatment for industrial wastes. J Hazard Mater 175:104–110

He M, Li X, Liu H, Miller SJ, Wang G, Rensing C (2011) Characterization and genomic analysis of a highly chromate resistant and reducing bacterial strain *Lysinibacillus fusiformis* ZC1. J Hazard Mater 185:682–688

Hu P, Brodie EL, Suzuki Y, McAdams HH, Andersen GL (2005) Whole-genome transcriptional analysis of heavy metal stresses in *Caulobacter crescentus*. J Bacteriol 187:8437–8449

Jin W, Zhang Z, Wu G, Tolba R, Chen A (2014) Integrated lignin-mediated adsorption-release process and electrochemical reduction for the removal of trace Cr(VI). RSC Adv 4:27843–27849

Joutey NT, Bahafid W, Sayel H, Ananou S, El Ghachtouli N (2014) Hexavalent chromium removal by a novel *Serratia proteamaculans* isolated from the bank of Sebou River (Morocco). Environ Sci Pollut R 21:3060–3072

Kamaludeen SP, Megharaj M, Juhasz AL, Sethunathan N, Naidu R (2003) Chromium-microorganism interactions in soils: remediation implications, reviews of environmental contamination and toxicology. Springer, pp. 93–164

Kapoor A, Viraraghavan T (1997) Heavy metal biosorption sites in *Aspergillus niger*. Bioresour Technol 61:221–227

Khambhaty Y, Mody K, Basha S, Jha B (2009) Biosorption of Cr (VI) onto marine *Aspergillus niger*: experimental studies and pseudo-second order kinetics. World J Microbiol Biotechnol 25:1413–1421

Kikuchi S, Kawauchi K, Kurosawa M, Honjho H, Yagishita T (2005) Non-destructive rapid analysis discriminating between chromium (VI) and chromium (III) oxides in electrical and electronic equipment using Raman spectroscopy. Anal Sci 21:197–198

Kılıç NK, Stensballe A, Otzen DE, Dönmez G (2010) Proteomic changes in response to chromium (VI) toxicity in *Pseudomonas aeruginosa*. Bioresour Technol 101:2134–2140

Krishna KR, Philip L (2005) Bioremediation of Cr (VI) in contaminated soils. J Hazard Mater 121:109–117

Megharaj M, Avudainayagam S, Naidu R (2003) Toxicity of hexavalent chromium and its reduction by bacteria isolated from soil contaminated with tannery waste. Curr Microbiol 47:0051–0054

Mohan D, Pittman CU Jr (2006) Activated carbons and low cost adsorbents for remediation of tri- and hexavalent chromium from water. J Hazard Mater 137:762–811

Myers C, Carstens B, Antholine W, Myers J (2000) Chromium (VI) reductase activity is associated with the cytoplasmic membrane of anaerobically grown *Shewanella putrefaciens* MR-1. J Appl Microbiol 88:98–106

Park D, Yun YS, Hye Jo J, Park JM (2005a) Mechanism of hexavalent chromium removal by dead fungal biomass of *Aspergillus niger*. Water Res 39:533–540

Park D, Yun YS, Park JM (2005b) Use of dead fungal biomass for the detoxification of hexavalent chromium: screening and kinetics. Process Biochem 40:2559–2565

Rai V, Khatoon S, Bisht S, Mehrotra S (2005) Effect of cadmium on growth, ultramorphology of leaf and secondary metabolites of *Phyllanthus amarus* Schum. and Thonn. Chemosphere 61:1644–1650

Ravindranath SP, Henne KL, Thompson DK, Irudayaraj J (2011) Surface-enhanced Raman imaging of intracellular bioreduction of chromate in *Shewanella oneidensis*. PLoS ONE 6:e16634

Saradhi PP, Mohanty P (1993) Proline in relation to free radical production in seedlings of *Brassica juncea* raised under sodium chloride stress. Plant Soil 155:497–500

Shen Y, Wang S, Tzou Y, Yan Y, Kuan W (2012) Removal of hexavalent Cr by coconut coir and derived chars—the effect of surface functionality. Bioresour Technol 104:165–172

Smutok O, Broda D, Smutok H, Dmytruk K, Gonchar M (2011) Chromate-reducing activity of *Hansenula polymorpha* recombinant cells over-producing flavocytochrome b_2. Chemosphere 83:449–454

Sultan S, Hasnain S (2007) Reduction of toxic hexavalent chromium by *Ochrobactrum intermedium* strain SDCr-5 stimulated by heavy metals. Bioresour Technol 98:340–344

Thacker U, Parikh R, Shouche Y, Madamwar D (2007) Reduction of chromate by cell-free extract of *Brucella* sp. isolated from Cr (VI) contaminated sites. Bioresour Technol 98:1541–1547

Theis T, Wedde M, Meyer V, Stahl U (2003) The antifungal protein from *Aspergillus giganteus* causes membrane permeabilization. Antimicrob Agents Ch 47:588–593

Vaskova H, Kolomaznik K (2013) Determination of trivalent and hexavalent chromium by Raman spectroscopy, Conference on Raman and Luminescence Spectroscopy in the Earth. Sciences, Austria

Xu L, Yang L, Luo M, Liang X, Wei X, Zhao J, Liu H (2011) Reduction of hexavalent chromium by *Pannonibacter phragmitetus* LSSE-09 coated with polyethylenimine-functionalized magnetic nanoparticles under alkaline conditions. J Hazard Mater 189:787–793

Yee N, Benning LG, Phoenix VR, Ferris FG (2004) Characterization of metal-cyanobacteria sorption reactions: a combined macroscopic and infrared spectroscopic investigation. Environ Sci Technol 38: 775–782

Zeng G, Chen A, Chen G, Hu X, Guan S, Shang C, Lu L, Zou Z (2012) Responses of *Phanerochaete chrysosporium* to toxic pollutants: physiological flux, oxidative stress, and detoxification. Environ Sci Technol 46:7818–7825